Macromolecules

ARTICLE

pubs.acs.org/Macromolecules

Dynamic Mechanical Behavior of Photo-Cross-linked Shape-Memory Elastomers

Jiahui Li, Christopher L. Lewis, Darcy L. Chen, and Mitchell Anthamatten*

Department of Chemical Engineering, University of Rochester, 206 Gavett Hall, Rochester, New York 14627-1066, United States

Supporting Information

ABSTRACT: Cross-linked elastomers containing reversibly binding side groups are capable of storing elastic energy on multiple time-scales, giving rise to shape-memory and self-healing properties. Photo-cross-linkable benzophenone side groups were incorporated into linear macromers containing reversible (2-ureido-4-pyrimidinone, UPy) side groups. This method enables melt-processing of shape-memory elastomers into complex permanent shapes, and samples can be prepared with much higher UPy-content. UV−vis spectroscopy was applied to study the efficacy of the cross-linking process. Resulting elastomer networks with variable densities of covalent cross-links and reversibly associating side groups were systematically prepared and studied. Dynamic mechanical analysis revealed the presence of two storage modulus plateaus: a high-temperature plateau attributed to covalent cross-links, and a lower temperature plateau attributed to both reversible and covalent cross-links. Results also show that dynamic cross-links behave nearly as effectively as permanent cross-links below the UPy hydrogen bond transition and that the presence of a covalent network supports cooperative binding of UPy side groups.

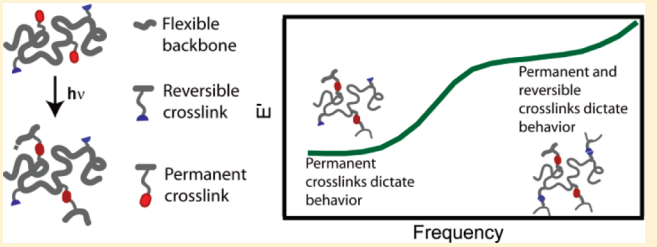

1. INTRODUCTION

Elastomers consist of macromolecular chains that are bound together into a network by covalent or noncovalent cross-links. Cross-links serve as permanent entanglements, restricting long-range and irreversible chain slippage. When deformed, chains are distorted from their most probable and preferable configurations, giving rise to an entropic restoring force.

A thermoresponsive shape-memory polymer (SMP) is capable of fixing a temporary shape when cooled, under elastic strain, beneath a well-defined shape-memory temperature (T_{SM}) that is often accompanied by crystallization or the formation of a polymer glass.[1−3] At temperatures beneath T_{SM}, the deformed shape is stabilized by the formation of crystalline or glassy domains, and this shape can be maintained indefinitely, even in the absence of stress. However, upon subsequent heating above T_{SM}, the SMP can be triggered to revert to its original shape as stored elastic strain-energy is recovered. Compared to shape-memory alloys and ceramics, SMPs are lightweight, relatively inexpensive, and the shape-recovery temperature can be adjusted through modification of polymer structure or architecture. Consequently, SMPs have received a great deal of research attention over the past decade.[4,5] Much effort has been devoted to improving shape fixity, increasing the recovery stress, and creating engineering materials that can recover extremely large (several hundred percent) strain.[6] Other notable developments included SMPs with multistaged recovery,[7,8] light-induced shape-recovery,[9] the ability to inductively heat particle-loaded materials using oscillating magnetic or electrical fields,[10,11] and the tailoring of biocompatible SMPs to meet specific biomedical needs such as sutures, stents, and catheters.[12]

In addition to crystallization and vitrification, dynamic transitions can also be used to stabilize mechanically deformed elastomers. We have previously shown that reversible hydrogen bonding can stabilize elastically deformed states. Specifically, poly(butyl acrylate) covalent networks containing 2-ureido-4-pyrimidinone (UPy) side groups were synthesized and studied.[13,14] The UPy group contains a linear array of four hydrogen bonding groups and undergoes self-dimerization with extraordinarily high solution dimerization constants (K_{dim} ~10^7 M^{-1} in $CDCl_3$).[15] A unique feature of these networks containing UPy side groups is that the rate of shape-recovery is adjustable and depends on temperature and the density of associating side groups. Moreover, the materials behave as elastomers both above and below the shape-memory transition temperature. Creep and rheology experiments of these and similar dynamic networks show Arrhenius-like temperature dependence, suggesting that mechanical relaxation is controlled by the rate of H-bond dissociation.[13,16] The integration of hydrogen bonding groups into soft materials has been extended to titin-mimicking modular polymers[17,18] and the concept of introducing both reversible and covalent cross-links has been applied to improve stress relaxation of coatings below the glass transition temperature.[19,20]

Here we demonstrate a new method of preparing shape-memory networks that utilize reversible association to temporarily stabilize mechanically deformed states. A series of linear

Received: February 21, 2011
Revised: May 26, 2011
Published: June 13, 2011

dx.doi.org/10.1021/ma2004019 | *Macromolecules* 2011, 44, 5336–5343

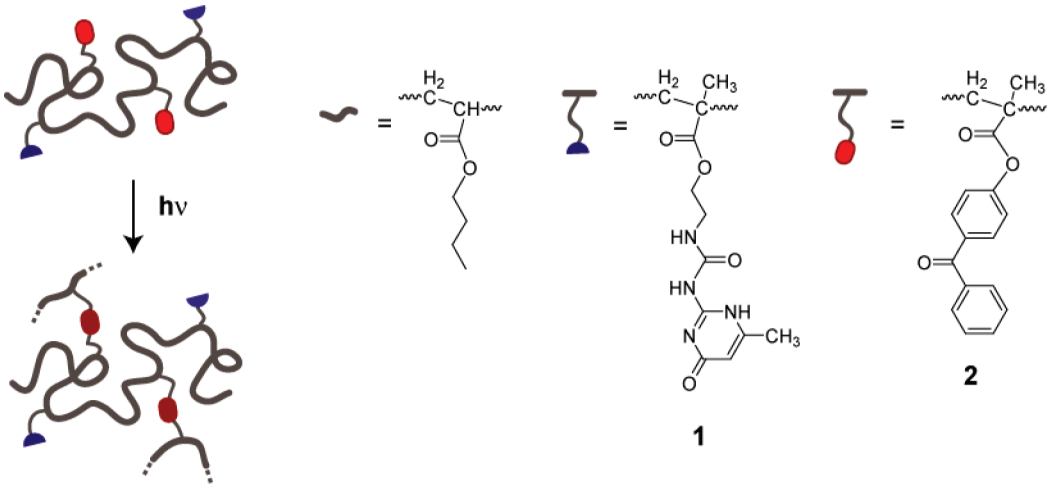

Figure 1. Scheme illustrating photo-cross-linking of network precursors to form dynamic networks containing both covalent and reversibly associating cross-links.

polymer melts containing different amounts of reversibly associating UPy groups and photo-cross-linkable side groups were synthesized and cross-linked using UV light (see Figure 1). This approach offers several advantages over the previously reported reactive-casting method.[13] Since linear polymers are prepared in solution, a greater density of hydrogen bonding side groups can be introduced into polymer networks, and more pronounced shape-memory effects are expected. Prior to cross-linking, linear polymers can be chemically characterized to properly deduce the composition of resulting networks. Network precursors can be molded into complex shapes that are defined by a transparent mold or a light pattern. Furthermore, since solvent removal is avoided, the network is formed near the stress-free state.[21]

In this study, macromers containing photosensitive benzophenone side groups (**2**) were synthesized. Benzophenone can undergo photolysis upon irradiation (a unimolecular process) followed by hydrogen extraction to form cross-links.[22,23] This manuscript addresses the efficacy of photo-cross-linking and the physical properties of formed networks. The resulting dynamic mechanical properties will be discussed and are related to the density of permanent and reversible cross-links with the goal of assessing the degree to which dynamic H-bond interactions act like permanent cross-links.

2. METHODS

Materials. All chemicals were reagent-grade and used without further purification. Butyl acrylate, 2-isocyonatoethyl methacrylate, 4-hydroxylbenzophenone, azobis(isobutyronitrile) (AIBN), triethyl amine, and deuterated chloroform ($CHCl_3$) were purchased from Aldrich. 2-amino-4-hydroxy-6-methylpyrimidine and methacryloyl chloride were purchased from Alfa Aesar. Solvents *N*-methylpyrrolidone (NMP), methanol, and dimethyl sulfoxide (DMSO) were purchased from Alfa Aesar. Solvent tetrahydrofuran (THF), $CHCl_3$ were purchased from J. T. Baker. THF and $CHCl_3$ used in this synthesis were purified using a Pure Solve PS-MD-3 solvent purification system from Innovative Technology. Coumarin derivatives are also known to dimerize upon exposure to UV light to form covalent cross-links (a bimolecular process).[24] Macromers containing Coumarin side groups were synthesized, however, thick films suitable for mechanical testing could not be achieved, and, therefore, experimental data are provided as Supporting Information.

Polymerization of Linear Macromers. Monomers 4-methacryloyloxy benzophenone[25] and ureidopyrimidinone ethyl methacrylate[26] were prepared according to the literature. A typical polymerization procedure to prepare macromers will be briefly described. In an air-free reaction flask, 80 mg (0.3 mmol) of 4-methacryloyloxy benzophenone, 164 mg (0.6 mmol) of ureidopyrimidinone ethyl methacrylate, and 3.84 g (30 mmol) of butyl acrylate were charged. Then, 4.8 mg of azobis(isobutyronitrile) (AIBN) was added as initiator, and 30 mL of $CHCl_3$ was added as solvent. After the mixture was degassed by N_2 bubbling for 0.5 h, the flask was immersed into a 75 °C oil bath and reacted overnight. The resulting polymer solution was precipitated in methanol, yielding a viscous liquid, yield =80%. ^{1}H NMR (Bruker 400) was used to determine the chemical compositions of the synthesized macromers. Molecular weight and polydispersity were measured by GPC (Agilent 1100) using THF as an eluent.

Photo-Cross-Linking of Macromer Films. Macromer solutions (~5 wt %, in chloroform) were cast onto quartz slides using a Teflon spacer with a 40 × 10 mm window. After solvent removal, the thickness of resulting films was about 0.5 mm. Films were placed into vacuum oven and dried overnight at 60 °C. Irradiation was conducted in a nitrogen glovebox to avoid oxygen inhibition. Samples were irradiated with a UV lamp (UVLM-28) with a measured intensity of 5 mW/cm^2 at 365 nm for 10 min increments. After each exposure, samples were held for 1 h to ensure free radical intermediates were consumed. The procedure was repeated until free radical intermediates were no longer observed using ultraviolet spectroscopy. Typically this required a total exposure time of 60 min.

Swelling and Gel Fraction Measurements. Weight and volume change were measured in triplicate for 0.5 mm thick specimens with an initial area measuring roughly 5 × 10 mm. Specimens were individually exposed to 15 mL of isopropyl alcohol (23 °C/48 h) and the sample mass and volume change recorded. Volume-swell is calculated according to the following relationship: $Q = 1 + (\rho_p)/(\rho_p)((M_{Swell})/(M_{Dry}) - 1)$ where Q is the volume swell (i.e., ratio of volume of swollen polymer to volume of dry polymer), ρ_s and ρ_p are the solvent and polymer densities, respectively, and M_{Dry} and M_{Swell} are the measured masses in the dry and swollen states, respectively. Specimens were subsequently dried in a vacuum oven at 80 °C for 48 h and weighed to determine gel fraction, expressed as the ratio of the final dry mass to the initial mass.

Dynamic Mechanical Testing. Photocured samples were cut into 6 mm ×10 mm films, and dynamic mechanical analysis was performed using a solid-state rheometer (Rheometrics, RSA-2). Frequency sweeps from 0.01 to 100 rad/s, at 2% strain, were acquired at

Table 1. Molecular Weight and Composition of Photo-Cross-Linkable Macromers

	cross-linker content		UPy content					
macromer	feed (mol %)	measd[a] (mol %)	feed (mol %)	measd[a] (mol %)	x_x[c]	x_{UPy}[c]	M_n[b]	PDI[b]
Bp1	1.0	0.70	0	0	5.6	0	104 000	1.14
Bp1-UPy1	1.0	0.78	1.0	0.6	5.8	4.4	96 400	1.21
Bp1-UPy2	1.0	0.77	2.0	1.7	5.9	12	98 800	1.22
Bp1-UPy5	1.0	1.10	5.0	6.4	3.5	19	42 500	1.82
Bp1-UPy10	1.0	0.86	10.0	11.8	3.6	49	61 400	1.77
Bp1/2-UPy2	0.5	0.54	2.0	2.1	2.6	10	62 100	1.39
Bp2-UPy2	2.0	1.65	2.0	2.5	5.4	8.2	43 000	1.72

[a] ^{1}H NMR. [b] GPC. [c] x_{XL} and x_{UPy} refer to average number of photo-cross-linkable (C*m*) and reversibly binding (UPy) side groups per macromer chain, respectively.

temperatures ranging from 30 to 100 °C at 10 °C increments. Storage modulus E', loss modulus E'' and tan δ were recorded at each experimental frequency and temperature. Data were analyzed using a commercial software package (TA Orchestrator v7) and time−temperature superposition was performed using a least-squares fitting routine (see Supporting Information).

3. DISCUSSION

3.1. Synthesis of Photo-Cross-Linkable Macromers. The characteristics of synthesized poly(butyl acrylate) macromers containing both UPy and photo-cross-linkable side groups are summarized in Table 1. The sample name specifies the mol % of the functional monomers in the feed: benzophenone (Bp), and ureidopyrimidinone (UPy). Macromers could be prepared with UPy-contents exceeding 10 mol %, and this is significantly higher than the UPy-content of prior shape-memory elastomers (~2 mol %).[13] Statistical copolymer compositions determined using ^{1}H NMR, agree fairly well with experimental feed compositions. Molecular weights, determined using GPC, ranged from 38 to 104 kDa—note that all copolymers exceed the entanglement molecular weight (~25 kDa) of poly(butyl acrylate).[27] The polydispersity indexes shown in Table 1 are lower than expected. It is suspected that this results from the removal of low molecular weight species during reprecipitation. For samples with high UPy-content, the polydispersity index was generally higher. For these samples, the presence of intermolecular UPy-UPy association may preclude the removal of low molecular weight species.

As seen in Table 1, each macromer chain contains between two and six benzophenone moieties. Only a fraction of available functional groups must be cross-linked to form an incipient gel. In the absence of cycle formation, gelation occurs when the average number of formed cross-links per primary chain exceeds $p_w/(p_w - 1)$ where p_w is the weight-average degree of polymerization. For high molecular weight polymers, p_w is large, and, therefore, on average, each chain requires just over one cross-link to form an incipient gel.[28]

Macromer **Bp1-UPy10** appeared to be a glassy polymer after precipitation and vacuum-drying. Solvent-casting resulted in stress accumulation and cracking during solvent removal; and macromer **Bp1-UPy10** was not photo-cross-linked. Further efforts to prepare quality **Bp1-UPy10** films for mechanical testing may involve slow solvent removal and thermal annealing.

3.2. Photo-Cross-Linking of Macromer Films. Macromers containing benzophenone side groups were cast into films and irradiated with a lamp measuring 5 mW/cm^2 at 365 nm. Hydrogen abstraction of benzophenone in polymer matrices has been well studied.[22,23,29] Through a two-photon process, the benzophenone group is excited to an $n\pi^*$ triplet state that abstracts a proton from the surrounding polymer matrix, forming a radical pair. The resulting ketyl radical recombines with the formed radical on the polymer matrix, resulting in a light-absorbing transient (LAT). The LAT has a distinct, long-lived UV absorption signature, and it further reacts to form stable photoproducts that are covalently bound to the surrounding polymer matrix.

Absorption spectra of macromer films, displayed in Figure 2, were obtained before and after UV exposures. Exposures were conducted in sequential 1, 2, 5 and 10-min periods. A characteristic absorption band at 333 nm was observed following exposure and is attributed to the LAT. The molar attenuation coefficient corresponding to the LAT band is 1.2×10^5 m^2/mol, and this is about 4 times that of the initial Bp coefficient. The observed band is similar to earlier reports of free benzophenone in substituted poly(methacrylate)s.[22,23] Following each exposure, films were held for a minimum of 1 h to allow photochemical intermediates to decay into stable photoproducts. The decay of the LAT band at 333 nm was studied, and the observed absorbance is plotted against time in Figure 2b. The half-life of this decay is about 8 min, and the rather high rate of decay is attributed to the low rigidity and low microviscosity of the poly(butyl acrylate) network.[23] The initial absorbance of the LAT band decreased following each irradiation period, indicating a reduction in the number of unreacted benzophenone side groups. UV exposures (10 min periods) were repeated until the LAT band was no longer observed, suggesting the film is fully cured. This typically required about eight exposure−decay cycles.

To ensure that UV exposure does not damage the poly(butyl acrylate) backbone, homopolymers were exposed to doses (10−100 J/cm^2) well beyond those used to cure benzophenone-containing polymers (~10−30 J/cm^2). The molecular weights of irradiated samples were measured using GPC. Even after an irradiation dose of 100 J/cm^2, the polymer's number-average molecular weight decreased by only about 10%. Additional experimental details and a plot of molecular weight versus irradiation dosage are available as Supporting Information.

Equilibrium volume-swell and gel fraction of cross-linked elastomers were measured by swelling in isopropanol followed by vacuum drying, and the results are presented in Table 2. Gel fractions all exceeded 90%, indicating the majority of chains were fixed to the cross-linked network. As expected, the gel fraction tended to be higher for samples with a high number of

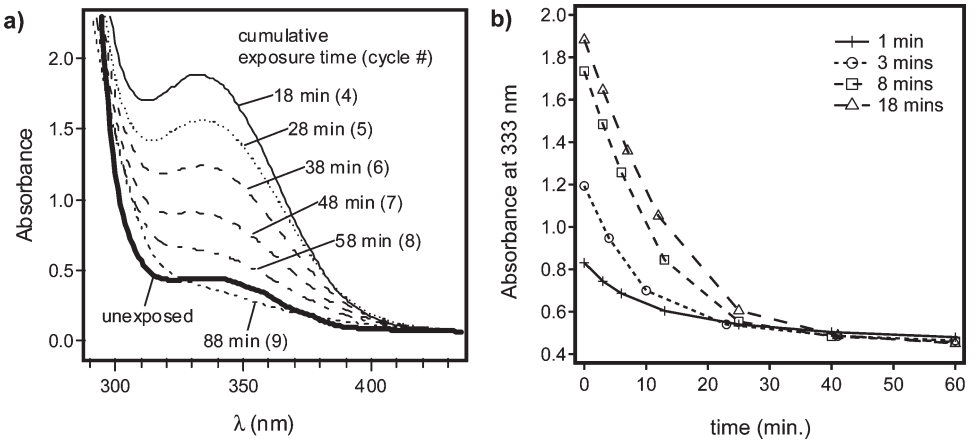

Figure 2. Photo-cross-linking of benzophenone-containing macromer **Bp1/2-UPy2**: (a) UV−vis spectra taken immediately after 10 min periods of UV periods—the absorption at λ = 333 nm indicates photo-cross-linking is incomplete; (b) absorbance maximum (at 333 nm) of the LAT decays following the end of each UV exposure period.

Table 2. Gel Fractions of UV-Cured Elastomers Determined from Swelling in Isopropyl Alcohol[a]

	gel fraction	Q
Bp1	98 ± 1.9	2.5 ± 0.17
Bp1-UPy1	100 ± 1.7	2.5 ± 0.02
Bp1-UPy2	98 ± 1.5	2.4 ± 0.09
Bp1-UPy5	93 ± 1.5	1.7 ± 0.04
Bp1/2-UPy2	91 ± 2.0	2.5 ± 0.04
Bp2-UPy2	96 ± 2.0	1.7 ± 0.06

[a] Data reported as mean ± one standard deviation.

benzophenone side groups per chain (x_x). For example, for **Bp-1-UPy1**, x_x = 5.8, and for **Bp1/2-UPy2**, x_x = 2.6. The volume swell did not appear to differ significantly for most of the samples investigated. A plot of volume swell versus strand density is provided as Supporting Information.

The shape-memory response of a typical sample (**Bp1/2-UPy2**) is shown in Figure 3. A flat, ribbon-like specimen (Figure 3a) was first wrapped around a mandrel at a sufficiently high temperature (65 °C) followed by submerging both the sample and mandrel into an ice water bath for approximately 1 min. The sample, now programmed into a corkscrew shape (Figure 3b), was then removed from the mandrel and blotted dry. At room temperature the programmed sample could be sustained over short times (Figure 3c), and the permanent shape appeared fully recovered after 48 h. Further, it was demonstrated that the shape-recovery time could be dramatically reduced by submersion of the programmed sample into hot water (65 °C) where the recovery process occurred in less than five seconds (Figures 3d−f). The strong temperature dependence of the shape−recovery process is not surprising and is a direct consequence of hydrogen bond exchange rate between temporary cross-links.[13] Dynamic mechanical analysis (DMA) will be discussed next to more fully characterize the thermo-mechanical behavior that gives rise to shape−memory effects.

3.3. Dynamic Mechanical Analysis of Dynamic Networks. *Elastic Energy Storage.* Photo-cross-linked benzophenone films were subjected to dynamic mechanical analysis. Frequency sweeps were performed at different temperatures, and resulting storage modulus measurements were shifted to yield the master

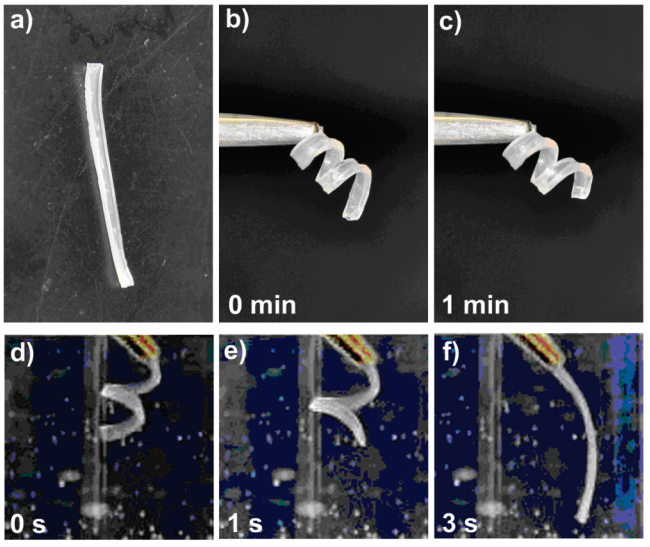

Figure 3. Demonstration of shape−memory response in **Bp1/2−Upy2**: (a) permanent shape (30 × 2 × 1 mm); (b) programmed, temporary shape immediately after forming; (c) temporary shape after 1 min in room temperature air; (d) temporary shape immediately following immersion in hot water (ca. 65 °C); (e) temporary shape after 1 s immersion in 65 °C water; (f) return to permanent shape occurs in approximately three seconds in 65 °C water. A video of the shape−memory response is included as Supporting Information.

curves shown in Figure 4. Samples with up to 2 mol % UPy content displayed two distinct plateaus (Figure 4a). The lower plateau modulus observed at low frequencies (10^{-4} to 10^{-2} Hz), corresponds to a network of covalent bonds created during photo-cross-linking. Evidently, the modulus of this plateau is proportional to the benzophenone content. The upper plateau, observed at higher frequencies ($10-10^{2}$ Hz) corresponds to the *overall* cross-link density—including both photo-cross-linked net points and reversible net points arising from the UPy dynamic network (Figure 5a). The highest storage modulus plateau of about 2.5 MPa was observed for **Bp2-UPy2**, bearing ~2 mol % of UPy and Bp side groups.

At higher UPy-contents, samples exhibit significantly higher storage modulus at all frequencies examined (see Figure 4b).

dx.doi.org/10.1021/ma2004019 |*Macromolecules* 2011, 44, 5336–5343

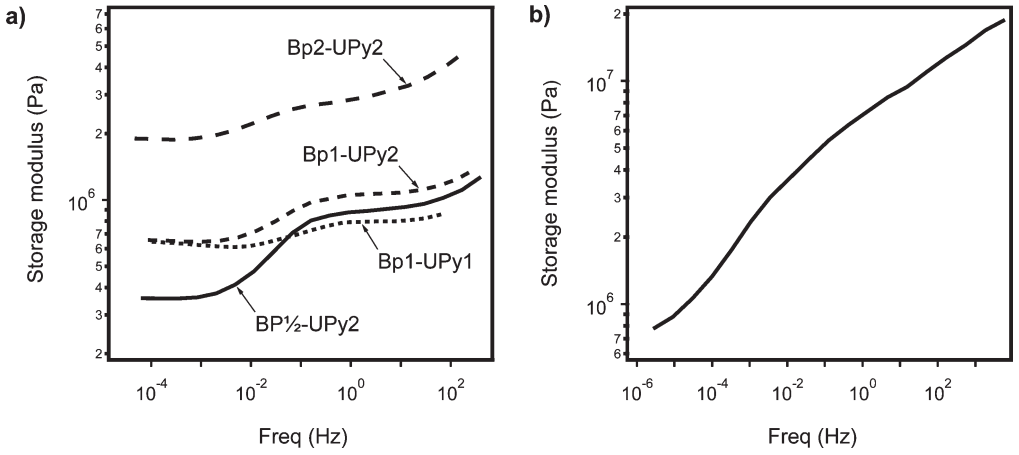

Figure 4. Storage modulus master curves for photo-cross-linked elastomers: (a) **Bp1/2-UPy2**, **Bp1-UPy1**, **Bp1-UPy2**, and **Bp2-UPy2**; (b) **Bp1-UPy5**. All data have been time−temperature superimposed to a 60 °C reference temperature.

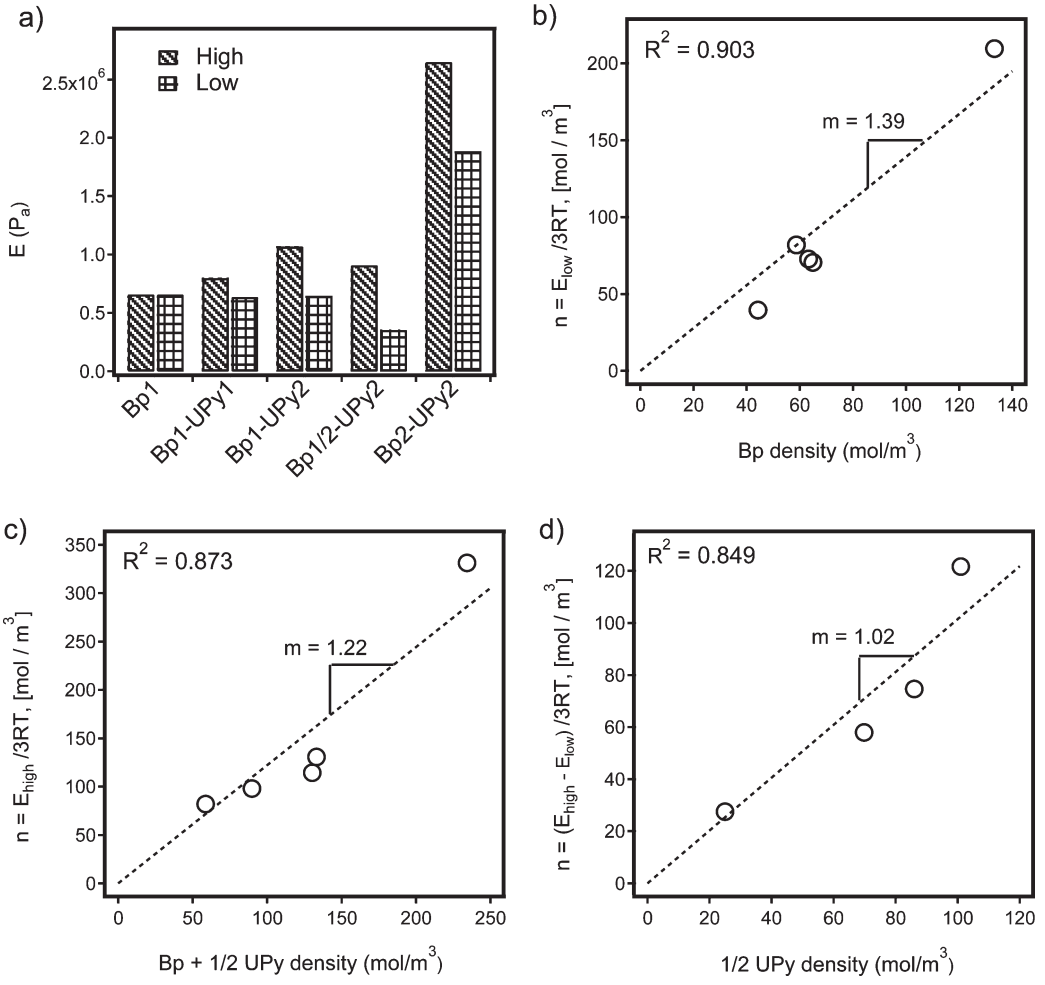

Figure 5. Relationship between plateaus in storage modulus and the composition of photo-cross-linked elastomers: (a) bar chart comparison between high and low plateaus of storage modulus for different compositions; (b) plot of strand density obtained from high temperature plateau modulus versus concentration of permanent cross-links based on Bp content; (c) plot of strand density obtained from low temperature plateau modulus versus total cross-link density based on Bp and UPy content; (d) plot of strand density attributed to UPy net-points versus UPy cross-link density.

The storage modulus of **Bp1-UPy5** at 1 Hz was about 8 MPa, nearly an order of magnitude higher than samples with lower UPy content at the same conditions. Moreover, the storage modulus for **Bp1-UPy5** increased strictly with frequency, over the range studied, and plateaus were not observed. The same hydrogen-bond transition is observed; however, it occurs at

dx.doi.org/10.1021/ma2004019 |*Macromolecules* 2011, 44, 5336–5343

lower frequencies, and it spans over a much broader range of frequencies. At low frequencies, the data appear to approach a plateau modulus similar to other samples with similar Bp content. The shift and broadening of the hydrogen-bond transition is attributed to cooperative dynamics which will be discussed later.

The classical theory of rubber elasticity can be applied to further understand how covalent and reversible cross-links affect storage modulus. Affine deformation of an ideal, incompressible elastomer results in a stress given by:

$$\sigma = nRT\left((1+\gamma) - \frac{1}{(1+\gamma)^2}\right) \quad (1)$$

where n is the number of strands per unit volume, R is the gas constant, T is temperature on an absolute scale, and γ is strain. In the limit of small strain, Hooke's law is valid, and the ratio of stress to strain (Young's modulus) becomes

$$E = 3nRT \quad (2)$$

Thus, if temperature dependence and chain-ends are neglected, each plateau modulus in Figure 4 corresponds to a different strand density n. The strand density corresponding to the lower plateau is plotted against the measured benzophenone concentration, *i.e.*, the maximum possible cross-link density, in Figure 5b. The data are fairly linear, and a least-squares fit through the origin results in a slope of ~1.4. According to the classical theory of rubber elasticity, if every benzophenone formed a tetrafunctional cross-link, then each cross-link would contribute two new strands to the network, and therefore a slope of two in Figure 5b is expected. The difference between the observed and theoretical slopes may arise from the following factors: (1) chain ends, which do not contribute to stored elastic energy, are present but are neglected; (2) chain connectivity is ignored; (3) not all benzophenone side groups may have reacted to form interchain cross-links. In light of these considerations, the data confirm that, upon irradiation, benzophenone groups successfully form chemical cross-links that influence mechanical properties in an expected and predictable way.

To examine whether reversible cross-links also behave as net points, the strand density corresponding to the upper plateau modulus is plotted against the overall cross-link density in Figure 5c. Since two UPy groups can dimerize to form a single interchain cross-link, the overall cross-link density is taken as the sum of the density of Bp side groups and one-half the density of UPy side groups. This choice of the abscissa results in a least-squares slope of 1.22 and a coefficient of determination of r^2 = 0.87. Plotting the same strand density against UPy density alone yields a poor correlation (r^2 = 0.46). Thus, the data indicate that both permanent and reversible cross-links contribute to the modulus at high frequency.

The fact the slope in Figure 5c is less than that in Figure 5b indicates that UPy dynamic cross-links are not as effective as Bp permanent cross-links. To further isolate the effectiveness of UPy cross-links, the data in Figure 5c were corrected by subtracting strand density contributions from permanent cross-links. Figure 5d displays the corrected strand density that is attributed to only UPy net-points versus UPy cross-link density. Least squares fitting results in a slope of 1.02, and, comparing this to the slope in Figure 5b suggests that, UPy cross-links are about 70% as effective as covalent cross-links at these concentrations. Furthermore, the data in Figure 5d are not linear. The slope increases with increasing UPy-content, indicating that UPy cross-links become more effective by increasing their concentration. This effect is attributed to cooperative dynamics, as will be discussed later.

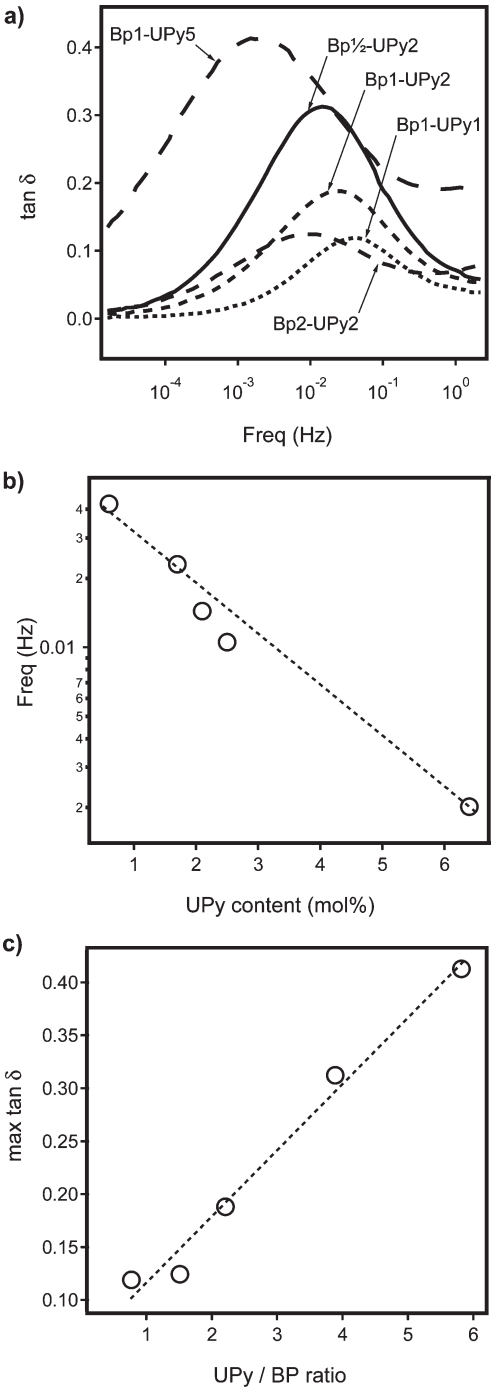

Figure 6. Influence of UPy-content on damping properties of photo-cross-linked elastomers: (a) tan δ master curves (using a reference temperature of 60 °C) of elastomers with different compositions, (b) tan δ peak frequency (at 60 °C) vs UPy content, and (c) the magnitude of the peak in tan δ versus the ratio of reversible to chemical cross-links.

Viscous Dissipation of Energy. In addition to the enhancement of the storage modulus, UPy side groups also significantly impact the materials' damping properties. Figure 6a shows time−temperature superimposed tan δ peaks for all photo-cross-linked samples containing UPy side groups. Both the magnitude and peak frequency of the loss-tangent depend on UPy-content.

dx.doi.org/10.1021/ma2004019 |*Macromolecules* 2011, 44, 5336–5343

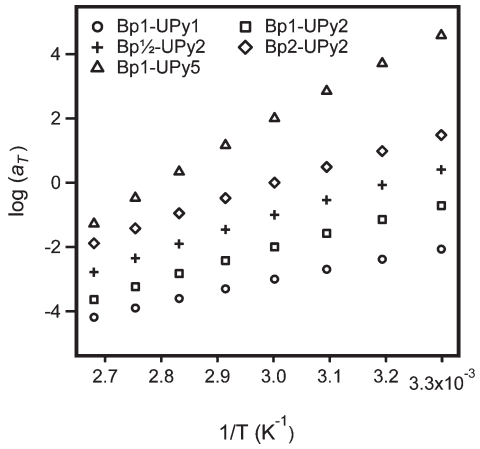

Figure 7. Shift factors for UPy-containing elastomers determined from time−temperature superposition of storage modulus using a reference of 60 °C. Data sets were shifted vertically to avoid overlap.

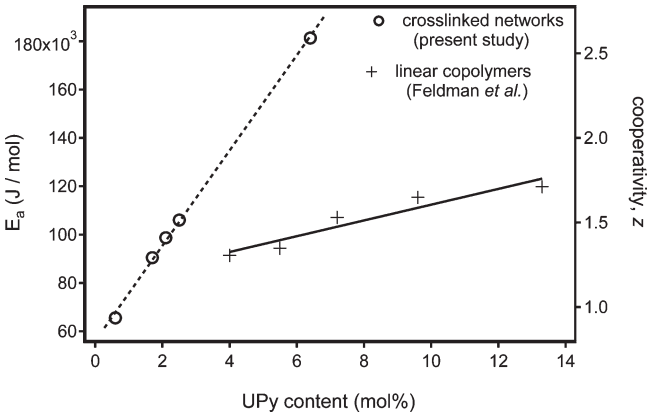

Figure 8. Plot of activation energies calculated from storage modulus shift factor versus measured UPy-content in photo-cross-linked elastomers.

As UPy-content increases, the damping peak shifts to lower frequencies (Figure 6b). At high frequencies less damping occurs because UPy dissociation events are too slow compared to the imposed strain frequency. At low frequencies the opposite occurs, and UPy bond dynamics are too fast to store and dissipate energy. The maximum viscous dissipation of energy occurs when the rate of chain relaxation, influenced by H-bond dynamics, nearly matches the experimental frequency. This frequency is nearly coincident with the inflection point of the storage modulus curves in Figure 4. Prior studies have indicated that H-bonding events in transient networks are correlated, resulting in slower dynamics for networks with higher concentrations of associating groups.[13,16,30] The correlated dynamics of UPy binding may explain the shift in the loss-tangent to lower frequencies with increasing UPy content observed in this study .

Figure 6c indicates that the magnitude of the loss-tangent peak is proportional to the molar ratio of UPy to Bp functional groups. UPy hydrogen bond dynamics influence the rate of chain relaxation by providing an additional mechanism to absorb energy. Enhanced frictional energy loss is attributed to continuous breaking and reforming of hydrogen bonds during the chain relaxation process giving rise to the observed relationship between tan δ and the number density of UPy groups. On the other hand, an increase in Bp concentration will yield an increase in storage modulus, which serves to reduce tan δ at a given UPy concentration. The ability of the UPy groups to increase material stiffness while also increasing the level of viscous energy dissipation provides an exception to the engineering trade-off between material stiffness and loss.[31]

Cooperativity of UPy Dynamics. UPy bond dissociation leading to mechanical stress relaxation is a thermally activated process that exhibits an Arrhenius-dependence on temperature.[13,14,16] Figure 7 shows how the shift factor, obtained when superimposing storage modulus curves, depends on inverse temperature for each dynamic network. As expected, the data are linear, confirming that UPy-dissociation leads to a loss of elastically stored energy and is thermally activated. The observed linearity is consistent with that observed in melts of random and triblock copolymers containing UPy side groups.[16]

The activation energies obtained from least-squares fits to the data in Figure 7 are plotted versus UPy-content in Figure 8. The activation energy depends linearly on UPy-content indicating that UPy dissociation dynamics are correlated. As a gauge for interpretation, the activation energy of UPy dissociation in chloroform determined using temperature-dependent NMR exchange spectroscopy is 70 ± 2 kJ/mol.[15] The energies in Figure 8 can be rescaled by this experimental value to yield a cooperativity factor, z (right-hand ordinate), that represents the average number of cooperative dissociation events required for an incremental loss in stored elastic energy. As a comparison, activation energies of UPy-containing random copolymers are also included in Figure 8.[16] The comparison shows that the activation energy is more sensitive to UPy-content in cross-linked networks than in linear copolymers. Thus, covalent cross-linking is an effective way to support the cooperative dynamics and bonding of reversibly associating groups.

■ CONCLUSIONS

A photo-cross-linking approach to preparing shape-memory elastomers bearing reversibly associating groups was demonstrated. Unlike solution-based approaches, photo-cross-linking is advantageous because: (i) macromer precursors can be thoroughly characterized using NMR and GPC techniques; (ii) the cross-linking process is solventless—avoiding stress accumulation that arises from solvent removal steps; (iii) a much greater fraction of H-bonding side groups can be achieved due to favorable solubility of the macromer; (iv) the technique provides the ability to tune the number density of both permanent and reversible cross-links. Synthesis involved conventional free radical copolymerization of butyl acrylate, a monomer containing a photoreactive benzophenone group, and a monomer containing the UPy side-group. Benzophenone-containing macromers are readily cross-linked upon UV exposure, and 500 μm-thick films were nearly completely cross-linked.

To understand how network architecture and reversible binding affects mechanical properties, photo-cross-linked elastomers containing benzophenone side groups were prepared with varying number density of permanent and dynamic cross-links. Dynamic mechanical analysis revealed two plateaus in the storage modulus master curves. A high-temperature plateau was attributed only to the permanent network, and the low-temperature plateau was attributed to both permanent and reversible cross-links. Moreover, a maximum in the loss tangent was observed that depends strongly on the UPy content. Higher UPy contents, and lower Bp contents, increased the magnitude of the damping (tan δ) peak,

while also enhancing the materials stiffness. Activation energies could be calculated from the temperature-dependence of shift factors obtained from time−temperature superposition of storage modulus curves. The activation energy was found to increase with UPy content, and this is consistent with cooperative dynamics of UPy binding. Finally, by comparing measured activation energies to those of linear UPy-containing polymers, the UPy binding effectiveness is clearly enhanced by covalent cross-links. Thus, in addition to providing mechanical support, covalent networks may be engineered to reinforce internal, complementary binding, and this idea may open new approaches to engineering shape−memory, self-healing, and other stimuli-responsive materials.

■ ASSOCIATED CONTENT

Supporting Information. (i) Example of ^{1}H NMR to determine copolymer composition; (ii) analysis of volume swell data; (iii) linear PBA degradation study; (iv) time−temperature superposition to obtain storage modulus master curves. (v) photo-cross-linking study of coumarin containing macromers; (vi) a video of the shape-memeory response. This material is available free of charge via the Internet at http://pubs.acs.org.

■ AUTHOR INFORMATION

Corresponding Author

*E-mail: anthamatten@che.rochester.edu. Telephone: (585)273-5526, fax: [585]273-1348.

■ ACKNOWLEDGMENT

The authors acknowledge support from funding provided by the National Science Foundation under Grant DMR-0906627. J. L. appreciates support from a Horton Fellowship administered through the Laboratory of Laser Energetics.

■ REFERENCES

(1) Liu, C.; Qin, H.; Mather, P. T. *J. Mater. Chem.* **2007**, *17*, 1543–1558.
(2) Mather, P. T.; Luo, X. F.; Rousseau, I. A. *Annu. Rev. Mater. Res.* **2009**, *39*, 445–471.
(3) Meng, Q. H.; Hu, J. L. *Composites, Part A: Appl. Sci. Manuf.* **2009**, *40*, 1661–1672.
(4) Behl, M.; Razzaq, M. Y.; Lendlein, A. *Adv. Mater.* **2010**, 3388–3410.
(5) Mather, P. T.; Luo, X.; Rousseau, I. A. *Annu. Rev. Mater. Res.* **2009**, *39*, 445−471.
(6) Voit, W.; Ware, T.; Dasari, R. R.; Smith, P.; Danz, L.; Simon, D.; Barlow, S.; Marder, S. R.; Gall, K. *Adv. Funct. Mater.* **2010**, *20*, 162–171.
(7) Luo, X. F.; Mather, P. T. *Adv. Funct. Mater.* **2010**, *20*, 2649–2656.
(8) Xie, T. *Nature* **2010**, *464*, 267–270.
(9) Lendlein, A.; Jiang, H. Y.; Junger, O.; Langer, R. *Nature* **2005**, *434*, 879–882.
(10) Koerner, H.; Price, G.; Pearce, N. A.; Alexander, M.; Vaia, R. A. *Nat. Mater.* **2004**, *3*, 115–120.
(11) Mohr, R.; Kratz, K.; Weigel, T.; Lucka-Gabor, M.; Moneke, M.; Lendlein, A. *P Natl Acad Sci USA* **2006**, *103*, 3540–3545.
(12) Small, W.; Singhal, P.; Wilson, T. S.; Maitland, D. J. *J Mater Chem* **2010**, *20*, 3356–3366.
(13) Li, J. H.; Viveros, J. A.; Wrue, M. H.; Anthamatten, M. *Adv. Mater.* **2007**, *19*, 2851–2855.
(14) Li, J. H.; Sullivan, K. D.; Brown, E. B.; Anthamatten, M. *Soft Matter* **2010**, *6*, 235–238.
(15) Soentjens, S. H. M.; Sijbesma, R. P.; van Genderen, M. H. P.; Meijer, E. W. *J. Am. Chem. Soc.* **2000**, *122*, 7487–7495.
(16) Feldman, K. E.; Kade, M. J.; Meijer, E. W.; Hawker, C. J.; Kramer, E. J. *Macromolecules* **2009**, *42*, 9072–9081.
(17) Kushner, A. M.; Vossler, J. D.; Williams, G. A.; Guan, Z. B. *J. Am. Chem. Soc.* **2009**, *131*, 8766–8768.
(18) Kushner, A. M.; Gabuchian, V.; Johnson, E. G.; Guan, Z. B. *J. Am. Chem. Soc.* **2007**, *129*, 14110−+.
(19) Wietor, J. L.; Dimopoulos, A.; Govaert, L. E.; van Benthem, R. A. T. M.; de With, G.; Sijbesma, R. P. *Macromolecules* **2009**, *42*, 6640–6646.
(20) Dimopoulos, A.; Wietor, J. L.; Wubbenhorst, M.; Napolitano, S.; van Benthem, R. A. T. M.; de With, G.; Sijbesma, R. P. *Macromolecules* **2010**, *43*, 8664–8669.
(21) Francis, L. F.; McCormick, A. V.; Vaessen, D. M.; Payne, J. A. *J. Mater. Sci.* **2002**, *37*, 4717–4731.
(22) Braeuchle, C.; Burland, D. M.; Bjorklund, G. C. *J. Phys. Chem.* **1981**, *85*, 123–127.
(23) Deeg, F. W.; Pinsl, J.; Braeuchle, C. *J. Phys. Chem.* **1986**, *90*, 5715–5719.
(24) Trenor, S. R.; Shultz, A. R.; Love, B. J.; Long, T. E. *Chem Rev* **2004**, *104*, 3059–3077.
(25) Toomey, R.; Freidank, D.; Ruhe, J. *Macromolecules* **2004**, *37*, 882–887.
(26) Yamauchi, K.; Lizotte, J. R.; Long, T. E. *Macromolecules* **2003**, *36*, 1083–1088.
(27) Zosel, A.; Ley, G. *Macromolecules* **1993**, *26*, 2222–2227.
(28) Dusek, K. Network Formation Involving Polyfunctional Polymer Chains. In *Polymer Networks: Principles of Their Formation Structure and Properties*; Stepto, R. F. T., Ed.; Blackie Academic & Professional: London, 1998; pp 64−92.
(29) Chilton, J.; Giering, L.; Steel, C. *J. Am. Chem. Soc.* **1976**, *98*, 1865–1870.
(30) Loveless, D. M.; Jeon, S. L.; Craig, S. L. *J Mater Chem* **2007**, *17*, 56–61.
(31) Lakes, R. S. *J. Compos. Mater.* **2002**, *36*, 287–297.